SANDIA REPORT
SAND2012-4905
Unlimited Release
Printed April 2012

CO_2-Based Mixtures as Working Fluids for Geothermal Turbines

Thomas M. Conboy, Steven A. Wright, David E. Ames, Tom G. Lewis

Prepared by
Sandia National Laboratories
Albuquerque, New Mexico 87185 and Livermore, California 94550

Sandia National Laboratories is a multi-program laboratory managed and operated by Sandia Corporation, a wholly owned subsidiary of Lockheed Martin Corporation, for the U.S. Department of Energy's National Nuclear Security Administration under contract DE-AC04-94AL85000.

Approved for public release; further dissemination unlimited.

Sandia National Laboratories

Issued by Sandia National Laboratories, operated for the United *S*tates Department of Energy by Sandia Corporation.

NOTICE: This report was prepared as an account of work sponsored by an agency of the United States Government. Neither the United States Government, nor any agency thereof, nor any of their employees, nor any of their contractors, subcontractors, or their employees, make any warranty, express or implied, or assume any legal liability or responsibility for the accuracy, completeness, or usefulness of any information, apparatus, product, or process disclosed, or represent that its use would not infringe privately owned rights. Reference herein to any specific commercial product, process, or service by trade name, trademark, manufacturer, or otherwise, does not necessarily constitute or imply its endorsement, recommendation, or favoring by the United States Government, any agency thereof, or any of their contractors or subcontractors. The views and opinions expressed herein do not necessarily state or reflect those of the United States Government, any agency thereof, or any of their contractors.

Printed in the United States of America. This report has been reproduced directly from the best available copy.

Available to DOE and DOE contractors from
U.S. Department of Energy
Office of Scientific and Technical Information
P.O. Box 62
Oak Ridge, TN 37831

Telephone: (865) 576-8401
Facsimile: (865) 576-5728
E-Mail: reports@adonis.osti.gov
Online ordering: http://www.osti.gov/bridge

Available to the public from
U.S. Department of Commerce
National Technical Information Service
5285 Port Royal Rd.
Springfield, VA 22161

Telephone: (800) 553-6847
Facsimile: (703) 605-6900
E-Mail: orders@ntis.fedworld.gov
Online order: http://www.ntis.gov/help/ordermethods.asp?loc=7-4-0#online

SAND2012-4905
Unlimited Release
Printed Jan 2012

CO_2-Based Mixtures as Working Fluids for Geothermal Turbines

Thomas M. Conboy
Steven A. Wright
Tom G. Lewis
David E. Ames

Advanced Nuclear Concepts
Sandia National Laboratories
P.O. Box 5800
Albuquerque, New Mexico 87185-1136

Abstract

Sandia National Laboratories is investigating advanced Brayton cycles using supercritical working fluids for application to a variety of heat sources, including geothermal, solar, fossil, and nuclear power. This work is centered on the supercritical CO_2 (S-CO_2) power conversion cycle, which has the potential for high efficiency in the temperature range of interest for these heat sources and is very compact—a feature likely to reduce capital costs. One promising approach is the use of CO_2-based supercritical fluid mixtures. The introduction of additives to CO_2 alters the equation of state and the critical point of the resultant mixture. A series of tests was carried out using Sandia's supercritical fluid compression loop that confirmed the ability of different additives to increase or lower the critical point of CO_2. Testing also demonstrated that, above the modified critical point, these mixtures can be compressed in a turbocompressor as a single-phase homogenous mixture. Comparisons of experimental data to the National Institute of Standards and Technology (NIST) Reference Fluid Thermodynamic and Transport Properties (REFPROP) Standard Reference Database predictions varied depending on the fluid. Although the pressure, density, and temperature (p, ρ, T) data for all tested fluids matched fairly well to REFPROP in most regions, the critical temperature was often inaccurate. In these cases, outside literature was found to provide further insight and to qualitatively confirm the validity of experimental findings for the present investigation.

Contents

1 Introduction 10

2 Benefits of Mixing – Cycle Analysis 12
2.1 CycleAnalysis© Code 12
2.2 Comparison of S-CO_2 Power Cycles with and without Additives 13

3 Experimental Work 22
3.1 Materials Compatibility 22
3.1.1 Procedure 22
3.1.2 Results 23
3.2 Turbocompressor Flow Loop Tests 24
3.2.1 Procedure 24
3.2.2 Results 26

4 Conclusions and Future Work 34

5 References 36

Figures

Figure 2-1. S-CO_2 Brayton cycle geothermal power cycle. 14
Figure 2-2. T-S diagram for the S-CO_2/butane working fluid mixture, with three stages of reheat and one stage of intercooling. 15
Figure 2-3. p-H diagram for the modified recompression S-CO_2 power cycle optimized for low-temperature applications. 15
Figure 3-1. Sandia materials screening autoclave. 22
Figure 3-2. Materials and component samples, post-test with 8% butane: a) AFLAS® gasket, showing signs of blistering, b) Armalon® sample, c) Sandia turbocompressor loop stator, and d) thermistors. 24
Figure 3-3. Schematic layout of the Sandia S-CO_2 compressor research loop. 25
Figure 3-4. Photograph of the Sandia S-CO_2 compressor research loop. 26
Figure 3-5. Observation of mass flow oscillations/noise at ~70ºF for a CO_2/8% butane mixture at 700kg/m^3. 27
Figure 3-6. Measured and REFPROP predicted saturation curve for schematic of the CO_2/8% butane mixture. 29
Figure 3-7: The p-T relationship for a 50/50 CO_2/SF_6 mixture at various densities, with experimental data shown at D=700 kg/m^3. 30
Figure 3-8. A comparison of the T-ρ NIST curves for CO_2 and SF_6, with acquired data. 31
Figure 3-9. Comparison of the p-T data for CO_2/4% Ne at 20 and 25 lb/ft^3 with NIST models. 32

Tables

Table 2-1. Comparison of S-CO_2 Power-Cycle Efficiency Using 1) the CO_2/10% Butane Mixture and 2) Pure CO_2 16
Table 2-2. Detailed Results for a S-CO_2 Recompression Brayton Cycle Using Three Stages of Reheat with One Stage of Intercooling and Only the Low-Temperature Recuperator 17
Table 3-1. Material Weight Change Following Screening Tests with Proposed Fluids..... 23

Nomenclature

DOE	U.S. Department of Energy
EERE	(DOE Office of) Energy Efficiency and Renewable Energy
EPDM	ethylene propylene diene monomer (M-class)
NIST	National Institute of Standards and Technology
REFPROP	Reference Fluid Thermodynamic and Transport Properties (NIST Standard Reference Database)
S-CO_2	supercritical CO_2

INTRODUCTION

Sandia National Laboratories (Sandia) is investigating advanced Brayton cycles using supercritical working fluids for application to a variety of heat sources, including geothermal, solar, fossil, and nuclear power. This work, under the Sandia and U.S. Department of Energy (DOE) Office of Advanced Reactor Concepts, is centered on the supercritical CO_2 (S-CO_2) power conversion cycle, which has the potential for high efficiency in the temperature range of interest for these heat sources and is very compact—a feature likely to reduce capital costs. As the S-CO_2 program progresses to a full Brayton power-generating cycle, new strategies are being pursued with a focus towards further pushing cycle efficiency.

One promising approach is the use of CO_2-based supercritical fluid mixtures [1]. The introduction of additives to CO_2 alters the equation of state and the critical point of the resultant mixture. Careful engineering of the working fluid enables the cycle to operate with a heat rejection temperature that is tailored to the local climate or day/night cycle at a given power plant, boosting overall conversion efficiency without the need for custom turbomachinery. The use of CO_2-based mixtures may be best suited to cycles operating in the low-temperature ranges characteristic of geothermal power. The current study is funded under the DOE Office of Energy Efficiency and Renewable Energy (EERE) to examine CO_2-based mixtures for advanced geothermal power cycles. The lower heat source temperatures are expected to lead to less dissociation or less cross-linking (coking) of gas molecules, which could affect the power system.

This report presents Sandia's recent research in the use of thermodynamic cycle modeling tools to improve the power cycle efficiency of low-temperature geothermal heat sources by using supercritical power cycles. The results of experiments performed in Sandia's supercritical fluid compression loop to test the ability of different additives to increase or lower the critical point of CO_2 are also presented.

BENEFITS OF MIXING – CYCLE ANALYSIS

The S-CO_2 development program at Sandia has developed a series of codes using CycleAnalysis© that can be used to model a variety of power cycles. Originally, the power cycle analysis tools focused on S-CO_2 as the working fluid. These tools relied on the National Institute of Standards and Technology (NIST) Reference Fluid Thermodynamic and Transport Properties (REFPROP) Standard Reference Database [2] to model the equations of state. In these early calculations, we observed that the critical point of CO_2 (as predicted by REFPROP) could be increased or decreased by adding in small quantities of other fluids.

Increasing the critical temperature was found to be useful in increasing the heat rejection temperature for S-CO_2 Brayton cycle systems. These early analyses showed, in general, that the decrease in efficiency that naturally occurs from higher heat rejection temperatures could be diminished by using CO_2 additives. The resulting increase in cycle efficiency was almost entirely due to the nonideal behavior of the fluid near the critical point. By increasing the ―effective" critical temperature, the power cycle could take advantage of the nonideal behavior (mainly compressor work) to increase the cycle efficiency. A DOE Technical Advance was filed to initiate the patent process for this discovery [3].

CycleAnalysis© Code

The CycleAnalysis© code is a Microsoft® Excel program that takes advantage of the Visual Basic programming language to predict the performance of a large number of closed power cycles for the supercritical fluid compression loop. Each power cycle is modeled under a separate tab within Excel. The code makes direct calls to the NIST REFPROP dynamic link library to perform the analysis. The code uses an enthalpy-based analysis method so it is not limited to fluids using ideal gas. The user supplies the compressor inlet temperature and pressure, the pressure ratio, the mass flow rate, and the isentropic efficiencies for the compressors and turbine. The code then calculates the state points (T = temperature, ρ = density, H = enthalpy, and S = entropy) at the inlet and outlet of each component within the loop. The code also assumes a pressure drop through all the components (typically 5% fractional pressure drop) for the entire loop. The code's solution method allows it to proceed through each component to find the inlet and outlet state points given a user-supplied approach temperature for the recuperators. Plots of the temperature-entropy (T-S) and pressure-enthalpy (p-H) diagrams are generated as are simple schematics of the power cycle. A summary section provides an output consisting primarily of the heater power, the gas-chiller heat rejection power, the power transferred in the recuperators, and the power within the compressor and turbines.

Each cycle includes an Excel solver that modifies the separate properties (pressure ratio, fraction of split flow, or compressor inlet pressure) to maximize the power cycle efficiency. The solver is also needed to ensure that the approach temperatures are within the user-specified bounds. The user can change the input values at any time, but not all inputs have solutions that are physical (primarily because the recuperators pinch or have reversed approach temperatures). Using the solver guarantees that the recuperator approach temperatures are physically real. It also ensures that they are within the user-specified input values.

Comparison of S-CO_2 Power Cycles with and without Additives

Figure 2-1 shows a schematic of a S-CO_2 power cycle that was developed to optimize efficiency for low-temperature geothermal heat sources. The cycle assumes that hot fluid is passed through three heaters to heat the CO_2 working fluid (with or without additives) and that the heat source is sufficiently hot that turbine inlet temperature can be heated to 433 K (160ºC). The proposed cycle also assumes that dry cooling, capable of cooling the compressor inlet temperature to 320 K (46.7ºC, 116ºF), is provided.

This power cycle is optimized to operate at low turbine inlet temperatures. The cycle is a modified recompression Brayton cycle that does not use the high-temperature recuperator; however, the waste cooling only uses a portion of the working fluid. This cycle is sometimes called the split-flow cycle because a fraction of the fluid is passed directly through a recompressor. (In essence, this recompression flow uses the recuperator as its waste heat rejection unit, but at a higher temperature than in the gas cooler.) To further increase efficiency, three stages of reheat and one stage of intercooling are provided. A summary of the temperatures and pressures and the power levels within each component are provided in Figure 0-1. The standard T-S and p-H diagrams are illustrated in Figures 2-2 and 2-3, respectively.

For this cycle, the predicted cycle efficiency is 18.1% when a 10 mole % mixture of butane and CO_2 is used. For comparison, the same cycle using pure CO_2 operates at a cycle efficiency of 14.5%. This 3.6 percentage point increase represents a 25% increase in cycle efficiency. This clearly shows the improvement that can be obtained by using CO_2 mixtures, or additives to CO_2, to tailor the working fluid to suit the environmental conditions in which it operates.

A detailed comparison of the pure CO_2 cycle and the CO_2/butane cycle mixture is provided in Table 0-1. For completeness, Table 0-2 presents all of the values calculated by the CycleAnalysis© code. Note that the Carnot cycle efficiency for this cycle is 26.1% and the CO_2/butane cycle efficiency operates at 69.1% of the Carnot efficiency.

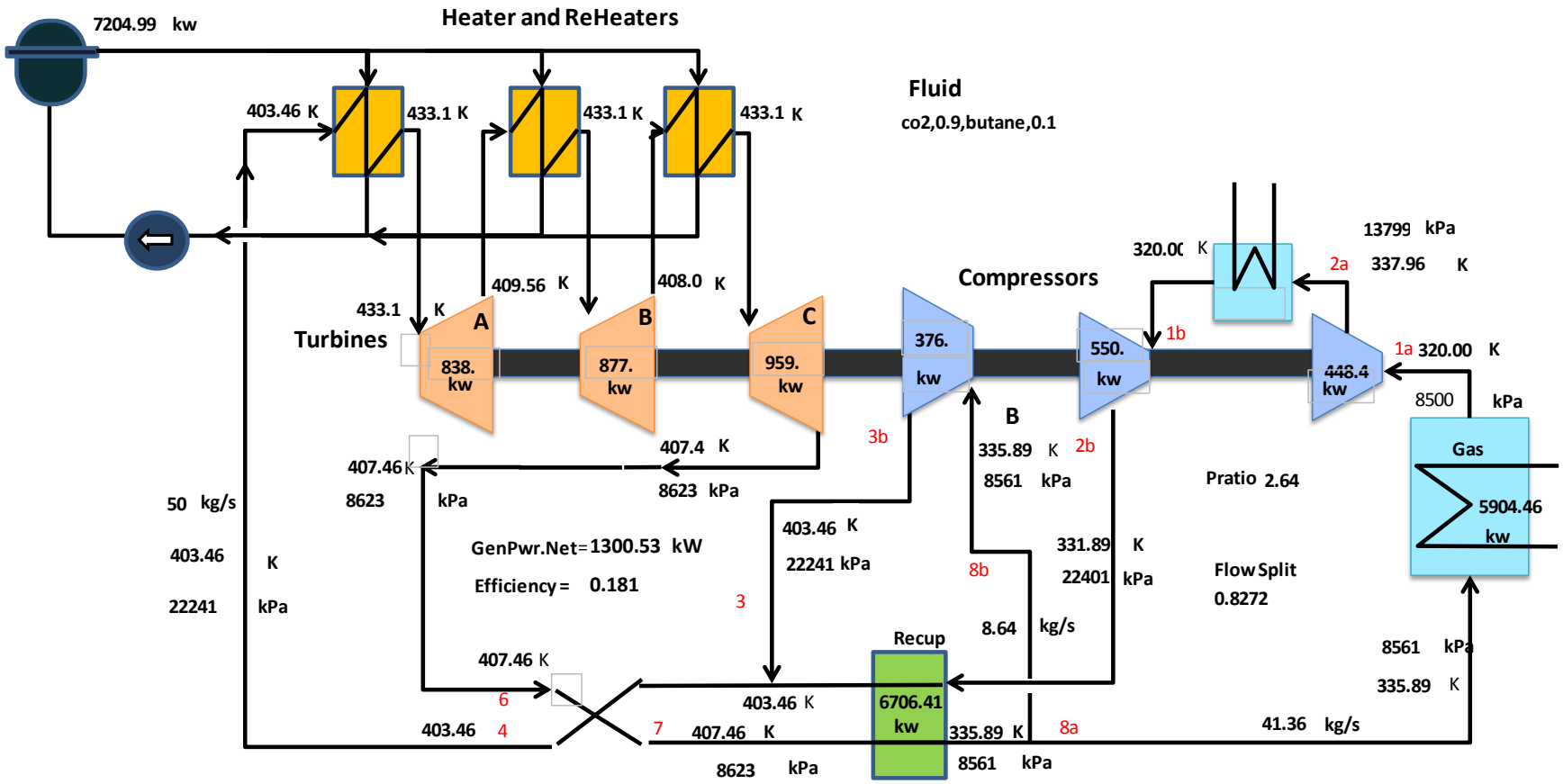

Figure 0-1. S-CO_2 Brayton cycle geothermal power cycle.
Turbine inlet T is 160ºC (433 K), with a dry cooling T of 46.7ºC (320 K) at the compressor inlet. The S-CO_2 cycle has three stages of reheat with one stage of intercooling. The power cycle is a modified recompression cycle that omits the high-temperature recuperator.

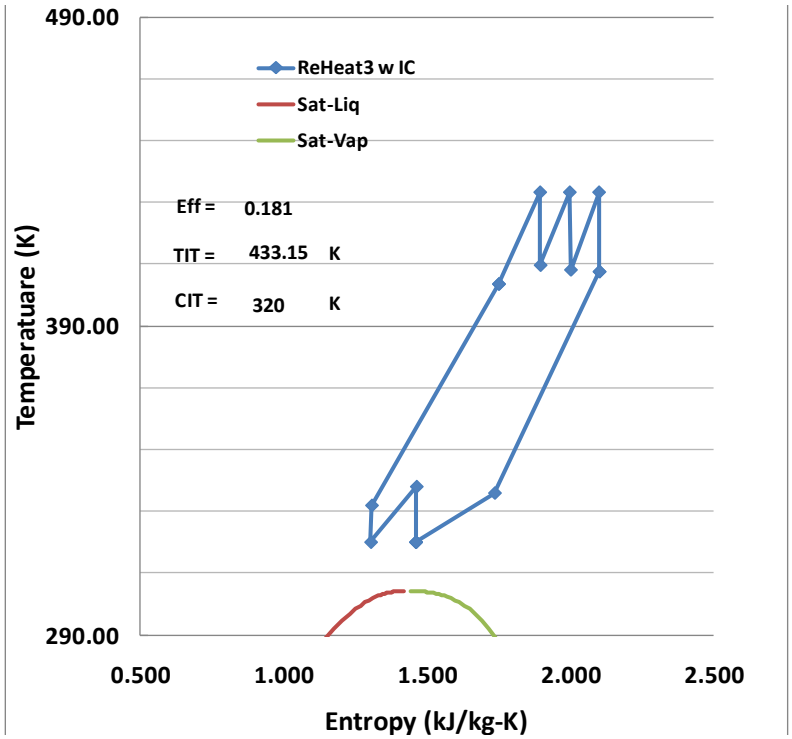

Figure 0-2. T-S diagram for the S-CO_2/butane working fluid mixture, with three stages of reheat and one stage of intercooling.

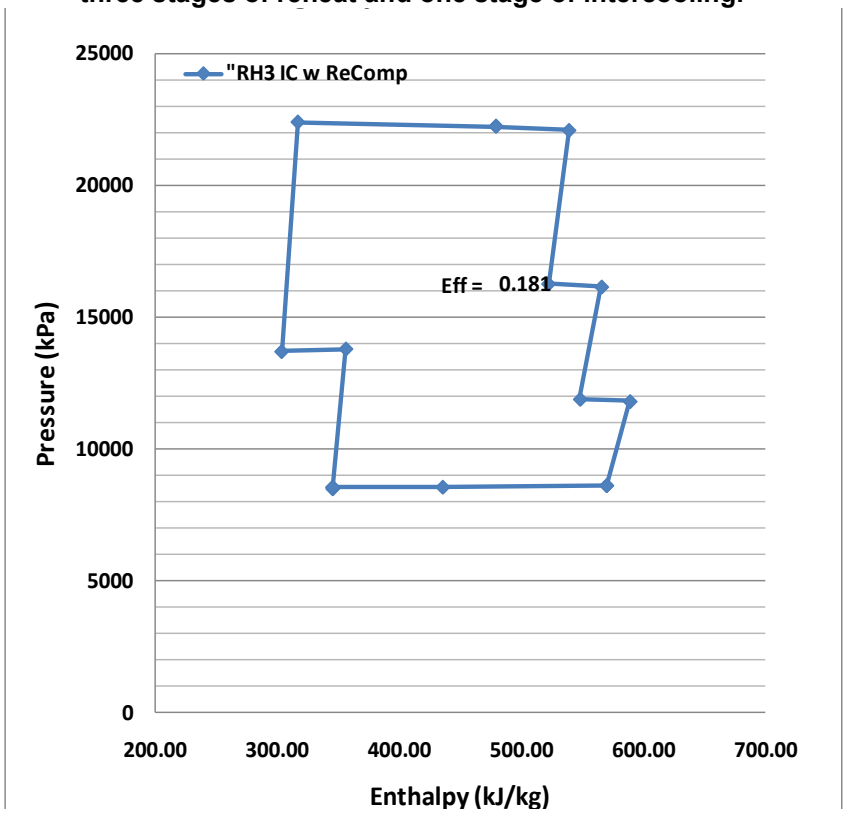

Figure 0-3. p-H diagram for the modified recompression S-CO_2 power cycle optimized for low-temperature applications.

Table 0-1. Comparison of S-CO_2 Power-Cycle Efficiency Using 1) the CO_2/10% Butane Mixture and 2) Pure CO_2

Parameter	Variable Name	CO_2/ 10% Butane	CO_2
Inlet Values			
Turbine Inlet T (K)	T.5	433.15	433.15
Fractional Pressure Drop	f.dp	0.0071	0.0071
Compressor Pressure Ratio	r.c	2.64	2.21
Compressor Inlet Pressure (kPa)	p.1	8500	8500
Compressor Inlet Temperature (K)	T.1	320	320
Mass Flow Rate (kg/s)	mdot	50	50
Split Flow Fraction through Chiller	f.split	0.83	0.61
Recuperator Approach Temperature (K)	dT.appr	4.00	4.00
Compressor Isentropic Efficiency	-	0.92	0.92
Recompressor Isentropic Efficiency	-	0.87	0.87
Turbine Isentropic Efficiency	-	0.97	0.97
Fraction of Carnot	-	0.69	0.56
Carnot Efficiency	-	0.26	0.26
Power (kW)			
Heat Transferred in HP Leg of LT Recuperator	-	6706.41	5234.17
Heat Transferred in LP Leg of LT Recuperator	-	6706.41	5234.17
Heat Transferred in HP Leg of HT Recuperator	-	0	0
Heat Transferred in LP Leg of HT Recuperator	-	0	0
Reactor Power (kW)	P.Rx	7204.99	5493.44
Main Compressor Power	P.Comp	448.39	444.74
Main Compressor Power B	P.Comp.B	550.24	300.62
Recompressor Power	P.ReComp	376.16	828.52
Turbine Power	P.turb	2675.32	2369.87
Chiller Heat Transfer	Q.Chill	5904.46	4697.44
TAC Power	P.TAC	1300.53	796.00
	P.TAC-chk	*1300.5*	*796.00*
Cycle Efficiency	-	0.18	0.15

Table 0-2. Detailed Results for a S-CO_2 Recompression Brayton Cycle Using Three Stages of Reheat with One Stage of Intercooling and Only the Low-Temperature Recuperator (Cycle Analysis Based on SNL's CycleAnalysis© code)

Parameter	Variable Name	Value
Inlet Values		
Turbine Inlet T (K)	T.5	433.15
Fractional Pressure Drop	f.dp	0.0071
Compressor Pressure Ratio	r.c	2.64
Compressor Inlet Pressure (kPa)	p.1	8500
Compressor Inlet Temperature (K)	T.1	320
Mass Flow Rate (kg/s)	mdot	50
Split Flow Fraction through Chiller	f.split	0.83
Recuperator Approach Temperature (K)	dT.appr	4.00
Compressor Isentropic Efficiency	-	0.92
Recompressor Isentropic Efficiency	-	0.87
Turbine Isentropic Efficiency	-	0.97
Fraction of Carnot	-	0.70
Carnot Efficiency	-	0.26
Main Compressor (kJ/kg-K)	s1a	1.46
Main Compressor (kg/m^3)	rho1	489.24
Compressor Inlet Density (kg/m^3)	rho1	489.24
Compressor Inlet Enthalpy (kJ/kg)	h1	345.50
Compressor Inlet Entropy (kJ/kg-K)	s1	1.46
Compressor Vdot (m^3/s)	vdot1	0.084
Main Compressor Out Pressure (kPa)	p.2	13798.90
Pure Isentropic Expansion (K)	T2s	337.70
Ideal Entropy Check (kJ/kg-K)	s2-ideal	1.46
Ideal Compressor Outlet Enthalpy (kJ/kg)	h2s	355.50
Ideal Change in Compressor Enthalpy (kJ/kg)	dHs	1.00
Actual Change in Compressor Enthalpy (kJ/kg)	dHactual	10.84
Actual Compressor Outlet Enthalpy (kJ/kg)	h2Actual	356.34
Compressor Outlet Temperature (K)	T2	337.96
Compressor Isentropic Efficiency	-	0.92
Entropy Compressor Out (kJ/kg-K)	s2	1.46
Density Compressor Out (kg/m^3)	d2	562.09
Enthalpy Compressor Out (kJ/kg)	h2	356.34
Compressor Power (kW)	p_comp	448.4

Table 2-2. Detailed Results for a S-CO_2 Recompression Brayton Cycle Using Three Stages of Reheat with One Stage of Intercooling and Only the Low-Temperature Recuperator (cont.)

Parameter	Variable Name	Value
Inter Cooler		
Inter Cooler Outlet T (K)	T1b	320
Inter Cooler Outlet Pressure (kPa)	p1b	13700
Inter Cooler Outlet Enthalpy (kJ/kg)	h1b	303.67
Inter Cooler Outlet Pressure (kg/m^3)	d1b	687.03
Inter Cooler Outlet Entropy (kJ/kg-K)	s1b	1.30
Power Inter Cooler (kW)	Pwr_IC	2178.34
Main Compressor b		
Main Compressor Out Pressure (kPa)	p.2b	22401
Pure Isentropic Compression (K)	T2bs	331.42
Ideal Entropy Check (kJ/kg-K)	s2b-ideal	1.30
Ideal Compressor Outlet Enthalpy (kJ/kg)	h2bs	315.94
Ideal Change in Compressor Enthalpy (kJ/kg)	dH2bs	12.27
Actual Change in Compressor Enthalpy (kJ/kg)	dHactual	13.30
Actual Compressor Outlet Enthalpy (kJ/kg)	H2bActual	316.98
Compressor Outlet Temperature (K)	T2b	331.89
Compressor Isentropic Efficiency	-	0.92
Entropy Compressor Out (kJ/kg-K)	S2b	1.30
Density Compressor Out (kg/m^3)	d2b	727.37
Enthalpy Compressor Out (kJ/kg)	h2b	316.98
Compressor Power (kW)	p_comp_b	550.24
Mass Flow in Main Compressor	-	41.36
Mass Flow in Recompressor	-	8.64
Pressures (kPa)		
Compressor A Inlet	p1a	8500
Compressor A Outlet	p2a	13799
Compressor B Inlet	p1b	13700
Compressor B Outlet	p2b	22401
Compressor C Outlet	p3	22241
Recup Outlet (Cold Leg)	p4	22241
Turbine A Inlet	p5a	22082
Turbine A Outlet	p6a	16262
Turbine B Inlet	p5b	16146
Turbine B Outlet	p6b	11891
Turbine C Inlet	p5c	11806
Turbine C Outlet	p6c	8623
Recup Inlet (Hot Leg)	p7	8623
Recup Outlet (Hot Leg)	p8	8561

Table 2-2. Detailed Results for a S-CO_2 Recompression Brayton Cycle Using Three Stages of Reheat with One Stage of Intercooling and Only the Low-Temperature Recuperator (cont.)

Parameter	Variable Name	Value
Turbines		
Turbine Intermediate Expansion Pressure (kPa)	p6a	16262
Turbine Inlet Entropy	s5a	1.90
Isentropic Temperature Turbine A Outlet	Ts6a	409.25
Should equal s5	-	1.90
Turbine Pressure Ratio	r.ta	1.36
Turbine Exit Temperature (K)	T6a	409.56
Turbine Isentropic Efficiency	-	0.96
Entropy Turbine A Inlet (kJ/kg-K)	s6a	1.90
Entropy Turbine B Outlet	s5b	2.00
Isentropic Temperature Turbine B Outlet	Ts6b	407.09
Temperature Turbine B Outlet	T6b	408.04
Entropy Turbine B Outlet	s6b	2.00
Entropy Turbine C Inlet	s5c	2.10
Isentropic Temperature Turbine C Outlet	Ts6c	407.00
Temperature Turbine C Outlet	T6c	407.46
		2.10
Enthalpy Turbine In (a) (kJ/kg)	h5a	538.87
Enthalpy Turbine Out (a) (kJ/kg)	h6a	522.10
Turbine Power (a) (kW)	P turb (a)	838.5
Enthalpy Turbine In (b) (kJ/kg)	h5b	565.62
Enthalpy Turbine Out (b) (kJ/kg)	h6b	548.07
Turbine Power (b) (kW)	P turb (b)	877.5
Enthalpy Turbine In (c) (kJ/kg)	h5c	588.90
Enthalpy Turbine Out (c) (kJ/kg)	h6c	569.72
Turbine Power (c) (kW)	P turb (c)	959.2
Turbine Total Power (a + b + c) (kW)	P turb (a+b+c)	2675.32
Chiller		
Gas Chiller Inlet Temperature (K)	T8	335.89
Gas Chiller Inlet Enthalpy (kJ/kg)	h8	435.59
Gas Chiller Inlet Entropy (kJ/kg-K)	s8	1.74

Table 2-2. Detailed Results for a S-CO_2 Recompression Brayton Cycle Using Three Stages of Reheat with One Stage of Intercooling and Only the Low-Temperature Recuperator (cont.)

Parameter	Variable Name	Value
Recompressor		
Recompressor Flow Rate (kg/s)	-	8.64
Ideal Compressor Temperature for Recompressor (K)	-	400.80
Should equal s8	-	1.74
Recompressor Outlet Temperature (K)	T3	403.46
Recompressor Isentropic Efficiency (K)	-	0.87
Recompressor Outlet Entropy (kJ/kg)	s3	1.75
Recompressor Outlet Density	d3	442.49
Recompressor Outlet Enthalpy (kJ/kg)	h3	479.13
Recompressor Power (W)	P_reComp	376.2
LT Recuperator		494.55
LT Recuperator LP Leg Inlet Enthalpy (kJ/kg)	h7	569.72
LT Recuperator LP Leg Inlet Temperature (K)	T7	407.46
(kJ/kg-K)	s7	2.10
Efficiency (1)	(T7–T8)/(T7–T2)	0.95
Efficiency (2)	(T3–T2)/(T7–T2)	0.95
Effectiveness of LT Recuperator	effLT recup	0.91
HT Recuperator		
Enthalpy HT Recuperator LP Leq Inlet (kJ/kg)	h6	569.72
Entropy of HT Recuperator LP Leg Inlet (kJ/kg-K)	s6	2.10
Enthalpy of HT Recuperator HP Leg Outlet (kJ/kg)	h4	479.13
Temperature of HT Recuperator HP Leg Outlet (K)	T4	403.46
Entropy of HT Recuperator HP Leg Outlet (kJ/kg-K)	s4	1.75
Efficiency of HT Recuperator	(T6–T7)/(T6–T3)	0.34
Effectiveness of HT Recuperator	effHT recup	0
Temperature at State Points		
Compressor A In (K)	T1a	320
Compressor A Out (K)	T2a	337.96
Compressor B In (K)	T1b	320
Compressor B Out (K)	T2b	331.89
Compressor C Out (K)	T3	403.46
HT Recuperator Cold Leg Out (K)	T4	403.46
Turbine A Inlet (K)	T5a	433.15
Turbine A Outlet (K)	T6a	409.56
Turbine B Inlet (K)	T5b	433.15
Turbine B Outlet (K)	T6b	408.04
Turbine C Inlet (K)	T5c	433.15
Turbine C Outlet (K)	T6c	407.46
HT Recuperator Hot Leg Out (K)	T7	407.46
Chiller Inlet (K)	T8	335.89

Table 2-2. Detailed Results for a S-CO_2 Recompression Brayton Cycle Using Three Stages of Reheat with One Stage of Intercooling and Only the Low-Temperature Recuperator (cont.)

Parameter	Variable Name	Value
Checks		
T8 > T2	-	LT Temps Bad
T7 > T3	-	HT Temps Okay
Should All Be Positive	T6–T4	4.00
Should All Be Positive	T7–T3	4.00
Should All Be Positive	T8–T2	4.00
Power		
Heat Transferred in HP Leg of LT Recuperator (kW)	-	6706.41
Heat Transferred in LP Leg of LT Recuperator (kW)	-	6706.41
Heat Transferred in HP Leg of HT Recuperator (kW)	-	0.00
Heat Transferred in LP Leg of HT Recuperator (kW)	-	0.00
Reactor Power (kW)	P.Rx	7205.99
Main Compressor Power (kW)	P.Comp	448.39
Main Compressor Power b (kW)	P.CompB	550.24
Recompressor Power (kW)	P.ReComp	376.16
Turbine Power (kW)	P.turb	2675.32
Chiller Heat Transfer (kW)	Q.Chill	5904.46
TAC Power (kW)	P.TAC	1300.53
	p.TAC-chk	1300.53
Efficiency Cycle	-	0.18
Densities		
Compressor Inlet Density (kg/m^3)	rho1	489.24
Compressor Outlet Density (kg/m^3)	rho2	562.09
Recompressor Outlet Density (kg/m^3)	rho3	442.49
Reactor Inlet Density (kg/m^3)	rho4	442.49
Turbine A Inlet Density (kg/m^3)	rho5a	365.50
Turbine A Outlet Density (kg/m^3)	roh6a	300.59
Turbine B Inlet Density (kg/m^3)	roh5b	260.39
Turbine B Outlet Density (kg/m^3)	roh6b	207.84
Turbine C Inlet Density (kg/m^3)	roh5c	180.69
Turbine C Outlet Density (kg/m^3)	roh6c	140.36
Main Recuperator LP Out Density (kg/m^3)	rh07	140.36
Recompressor Inlet Density (kg/m^3)	rh08	259.94

EXPERIMENTAL WORK

Materials Compatibility

Procedure

Additive fluids were selected for testing based on their anticipated changes to the CO_2 critical temperature, but also based on their perceived low risk for corrosion or other damage to turbomachinery and loop materials. The compatibility of the fluid mixtures with the loop structural materials and gaskets needed to be verified before operation. This verification was performed in an autoclave test chamber (see Figure 3-1) for the following mixtures (% mole): CO_2/10% He, CO_2/10% Ne, CO_2/19% methane, CO_2/8% n-butane, and 100% pure SF_6. Methane and butane mixture ratios were selected based on known flammability limits for alkane mixtures with CO_2.

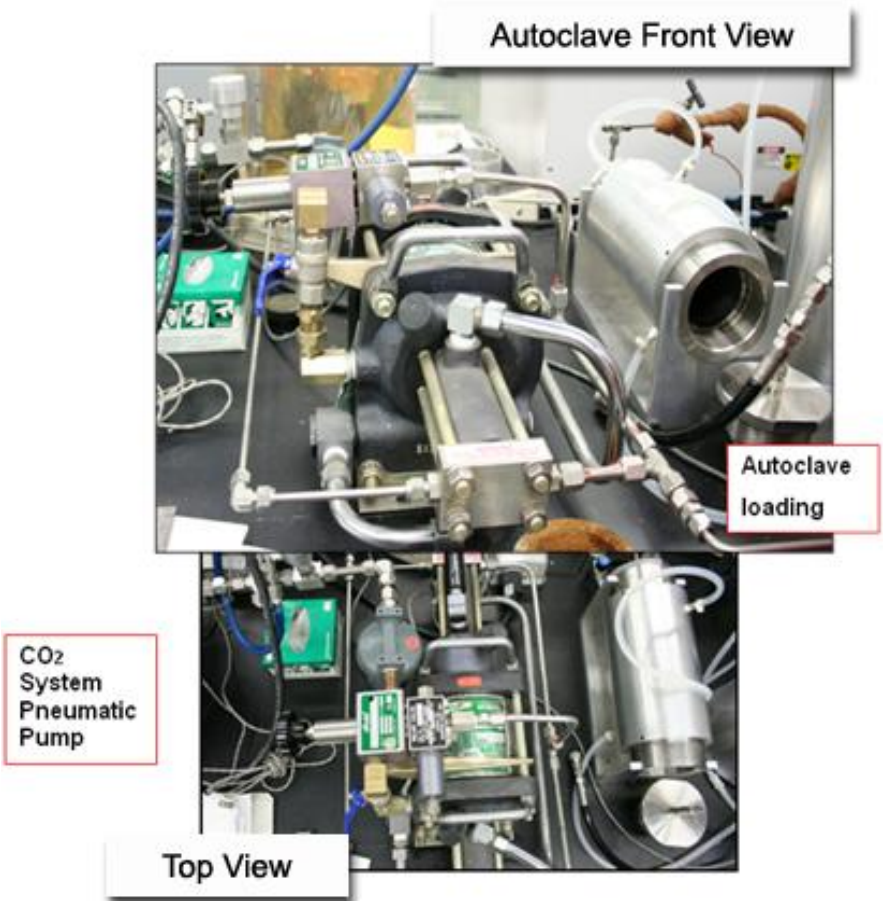

Figure 0-1. Sandia materials screening autoclave.

For these compatibility tests, the additive fluids were selected to be at or in excess of their mole fraction intended for use within the test loop. Material samples selected were those used in Sandia's supercritical fluid compression loop or other candidate materials for future systems. This included: 1) samples of O-ring materials—EPDM (ethylene propylene diene monomer (M-class)), AFLAS®, and Viton®; 2) dry lubricants—Turcon® and Armalon®; 3) a stator similar to that used in the compression loop; and 4) several thermistors.

Each sample was placed in the autoclave and exposed to the respective CO_2-based mixture for two weeks at approximately 1100 psi and 40°C (for pure SF_6, which has a lower critical pressure, testing was done at 580 psi and 50°C). This low-temperature study is by no means a comprehensive compatibility screening, but was used to determine whether each fluid was unlikely to damage Sandia's supercritical fluid compression loop over the short term at temperatures below 50°C.

Results

Table 0-1 shows a summary of the findings. Aside from small changes in weight, no major changes to material properties were observed in this test matrix. In several cases, the AFLAS® gasket showed signs of minor blistering (see Figure 3-2). This was thought to be due to infiltration of the CO_2/mixture over the test period, followed by explosive decompression, as the chamber pressure was lowered at the conclusion of the test. Because AFLAS® is not actively used in the loop, this did not pose a concern.

Table 0-1. Material Weight Change Following Screening Tests with Proposed Fluids

Material/ Component	CO_2/ 10% He	CO_2/ 10% Ne	100% SF_6	CO_2/ 8% Butane	CO_2/ 19% Methane
EPDM	-0.72%	-3.60	-2.13	-7.25	+0.10
AFLAS®	+1.47%	+0.00	+4.38	+3.16	+0.74
Viton®	-0.61%	-1.20	+6.79	+2.57	+0.40
Turcon®	-2.57%	+0.71	+4.88	+1.22	-0.61
Armalon®	+0.00%	+0.00	+0.15	+0.01	-0.02
SNL stator	+0.00%	+0.03	+0.00	+0.05	-0.04
SNL thermistors	n/a	n/a	n/a	+0.41	+0.30

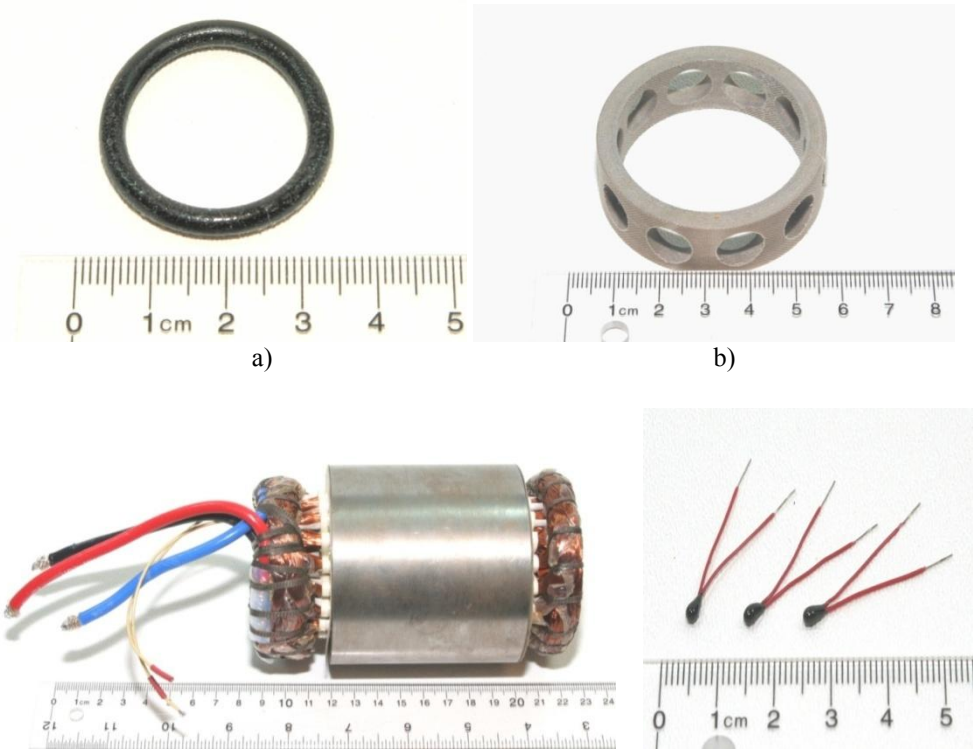

Figure 0-2. Materials and component samples, post-test with 8% butane: a) AFLAS® gasket, showing signs of blistering, b) Armalon® sample, c) Sandia turbocompressor loop stator, and d) thermistors.

Turbocompressor Flow Loop Tests

Procedure

A schematic diagram of Sandia's supercritical fluid compression loop is presented in Figure 3-3. Temperature and pressure state points are measured at the entrance and exit of each major component, as indicated on the figure as 1) compressor inlet, 2) compressor outlet, 3) heater outlet, and 4) expansion valve outlet. Mass flow and density are measured at the compressor inlet using a coriolis flow meter. A remote-controlled expansion valve is used to vary the mass flow around the loop, enabling the evaluation of compressor performance characteristics.

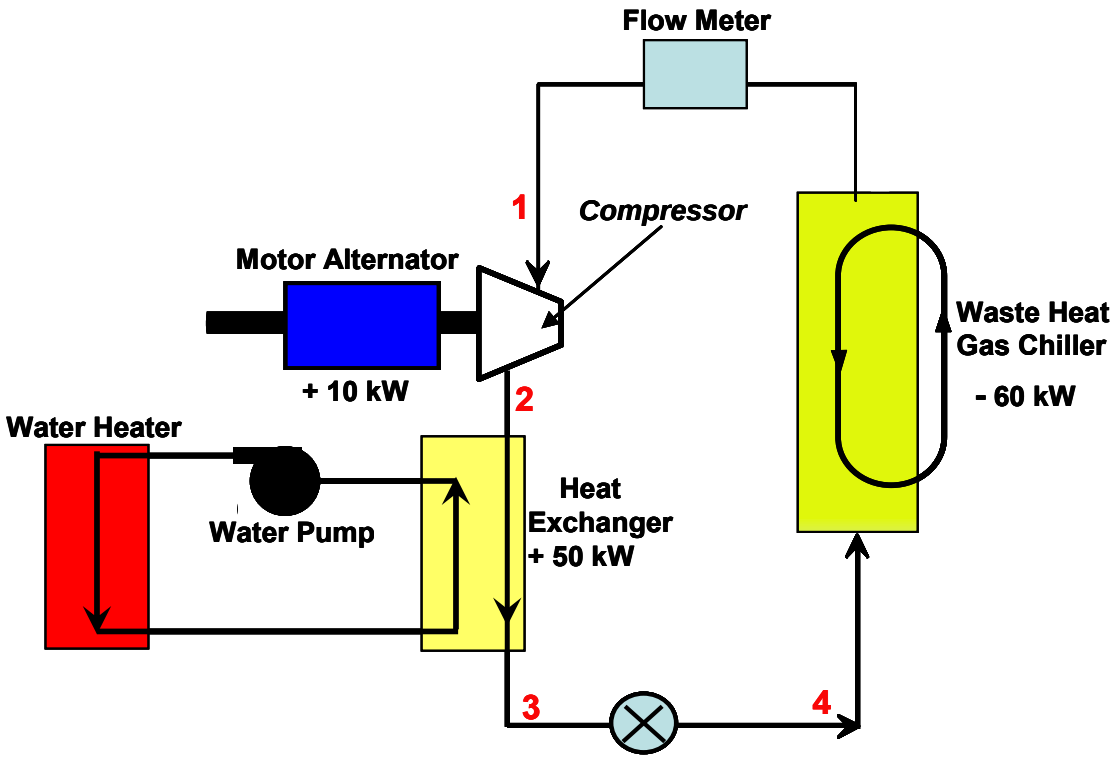

Figure 0-3. Schematic layout of the Sandia S-CO_2 compressor research loop.

The supercritical fluid compression loop was fabricated by Barber Nichols, Inc. of Arvada, CO, under contract to Sandia. It is constructed primarily of 304 and 316L stainless steels, and has a maximum allowable working pressure of 18 MPa (2600 psi) at 820 K. The loop uses a 50-kW_e motor driven compressor capable of spinning the compressor at design speeds up to 75,000 rpm with a pressure ratio of 1.8 and a flow rate of 3.53 kg/s for a compressor inlet condition of 305.3 K (89.87°F) and 7.690 MPa (1115 psi). More details regarding this facility can be found in Wright [4]. A photograph of the loop is shown in Figure 3-4.

The loop was initially developed to study the compression of CO_2 near the critical point. Subsequent tests have used the same turbomachinery, unmodified, to investigate off-nominal conditions, including CO_2 compression in the liquid and gas phases and in the two-phase saturation region. Alternative pure supercritical fluids, such as SF_6, have also been tested experimentally in this facility. These recent tests using supercritical-mixture working fluids are only the latest in a series exploring operation away from compressor design conditions.

Figure 0-4. Photograph of the Sandia S-CO_2 compressor research loop.

There were several aims for this experimental work, as follows:

1) *Mixture Equation of State:* For thermodynamic cycle analysis and data reduction, Sandia has developed tools that rely on dynamic links to the NIST REFPROP. In many cases in which previous experimental work is limited, REFPROP is unproven for determining mixing parameters. Therefore, it was necessary to chart experimental equation of state (p, ρ, T) data for comparison with NIST models.

2) *Mixture Critical Point:* In earlier testing with pure CO_2, it was discovered that one could roughly determine the saturation curve of a fluid, and consequently its critical temperature, by observing the onset of minor mass flow oscillations and density oscillations that occur as the boundary is approached (indicative of a two-phase flow instability). Comparison of the experimentally-observed mixture critical points to REFPROP predictions was also an important objective.

3) *Compressor Performance:* Finally, it was necessary to verify stable compressor operation using supercritical mixtures and to acquire pressure ratio versus mass flow data that could later be used to map compressor performance. This was accomplished by running the compressor at a fixed speed while incrementally closing the expansion valve, which would drive up compressor outlet pressure. Speeds of 35, 40, 45, and 50 krpm were examined with varying expansion valve settings.

Results

To date, full-scale compressor tests using the supercritical fluid compression loop have included CO_2/8% mole n-butane, CO_2/4% mole neon, and CO_2/SF_6 mixtures in mass ratios of 30/70, 40/60, and 50/50. These tests first consisted of running the compressor at 25 krpm while varying

the loop temperature to examine equation of state. Then, excursions from 25 to 50 krpm were made in increments of 5 krpm at various pressure ratios to accumulate data for compressor maps.

***CO_2/Butane*:**

Mixtures of CO_2/8% butane were tested in the flow loop at densities of ~160, 350, 460, 580, and 700 kg/m^3. At each fill density, loop temperature was varied from ~290 to 320 K (65 to 115°F) using heaters and cooling flow as needed with the compressor operating steadily at 25 krpm. The onset of flow oscillations was observed at a unique temperature for each new density (or entropy) investigated. This can be seen in Figure 0-5 for the case of a 700 kg/m^3 fill density: T400, 500, 600, and 200 correspond to state points 1, 2, 3, and 4 of Figure 0-3 (temperatures at the compressor inlet, outlet, heater outlet, and expansion valve outlet, respectively). As the loop is slowly cooled to ~70ºF (294 K) at all points, noise suddenly appears in the previously steady mass flow data. The mass flow stabilizes as heating is reapplied to lift the system back above the saturation region, and remains steady as more heat is added progressively. This clearly indicates a transition from single-phase to two-phase at 70ºF for a density of 700 kg/m^3.

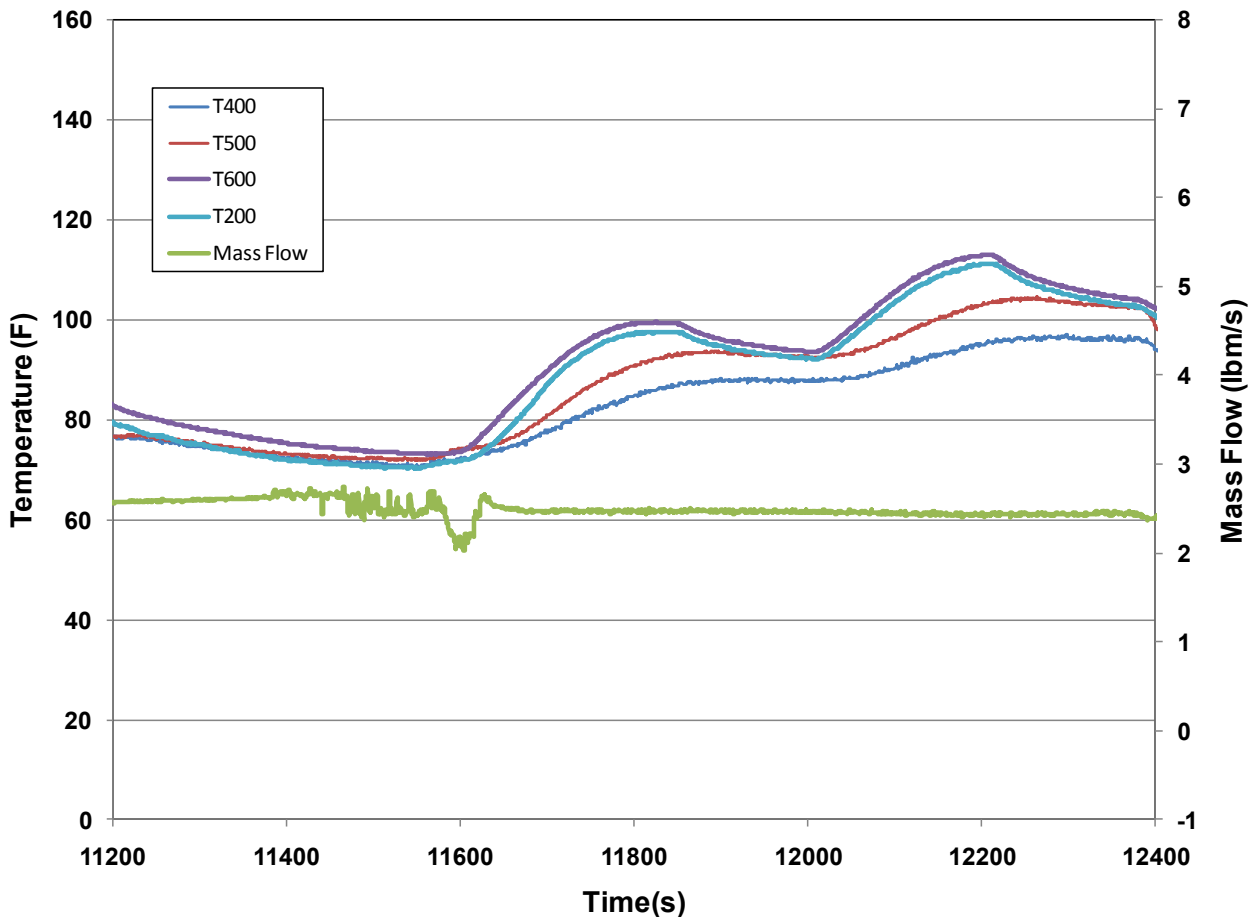

Figure 0-5. Observation of mass flow oscillations/noise at ~70ºF for a CO_2/8% butane mixture at 700kg/m^3.

By carrying out this procedure at a number of different fill densities, one can roughly trace the two-phase saturation curve for the fluid mixture. This is shown in Figure 0-6; the phase transition data from CO_2/butane at five different densities was plotted and fit with a polynomial curve to show a comparison between measured compressor loop data and NIST modeling.

In Figure 0-6, the blue points and curve represent experimental data, and the black background lines show curves reported by REFPROP. Error bars drawn on the experimental data indicate the variation of temperatures around the loop at the point of phase transition (not measurement error), which is on the order of ±1.1 K for the K-type thermocouples used. The major uncertainty is caused by the loop not being totally isothermal, as small temperature differences (1–2 K) existed around the loop. The orange dotted line shows the critical temperature of pure CO_2, at 88°F (304 K). As seen, the measured curve was found to be close to, but several degrees lower than, NIST predictions.

The data confirms a modified critical point near 104°F (313 K), as a result of the added butane. This is not far off from NIST estimates, which place the modified critical point at 316 K. In fact, predictions for CO_2/butane were, on the whole, quite reliable. This is a result of a large base of butane-mixture experimental data and models that are available in literature from the natural gas industry and that are incorporated within REFPROP [5]. Equation of state data agreed well between this experiment and REFPROP at nearly all points.

CO_2/SF_6:

The CO_2/SF_6 mixture tests were handled differently from the CO_2/butane tests, in that the two fluids were combined ~~–b~~y hand" in the lab rather than preordered as a custom mixture. Consequently, gas added into the loop was measured by mass using a laboratory scale, and mixtures are reported as mass ratios. Ratios of 30/70, 40/60, and 50/50 were tested (equivalent to ranges of ~25–40% SF_6 by mole fraction).

Comparison of equation of state data for the CO_2/SF_6 mixtures to REFPROP predictions yielded good agreement above the critical point. For each test case, working fluid temperature was lowered from ~320 to 300K (115 to 80°F) to allow for the observation of the pressure response. Figure 0-7 shows the comparison of data for a 50/50 mixture at 700 kg/m^3; excellent agreement is observed between NIST predictions (in green) and the experimental data (in blue). This is not trivial, as REFPROP does not base models on experimental data for CO_2/SF_6. Instead, the user is warned that mixing parameters are unavailable and will be estimated. For CO_2/SF_6, the code uses a default model based on refrigerant fluid mixtures [6].

However, the critical point predicted by REFPROP was not close to the experimental value. Pure SF_6 has a critical temperature near 319K (115°F), and CO_2 has a critical temperature at 304 K (88°F); knowing little about the interaction between these molecules, one might expect the mixture to have a critical temperature somewhere between these two values.

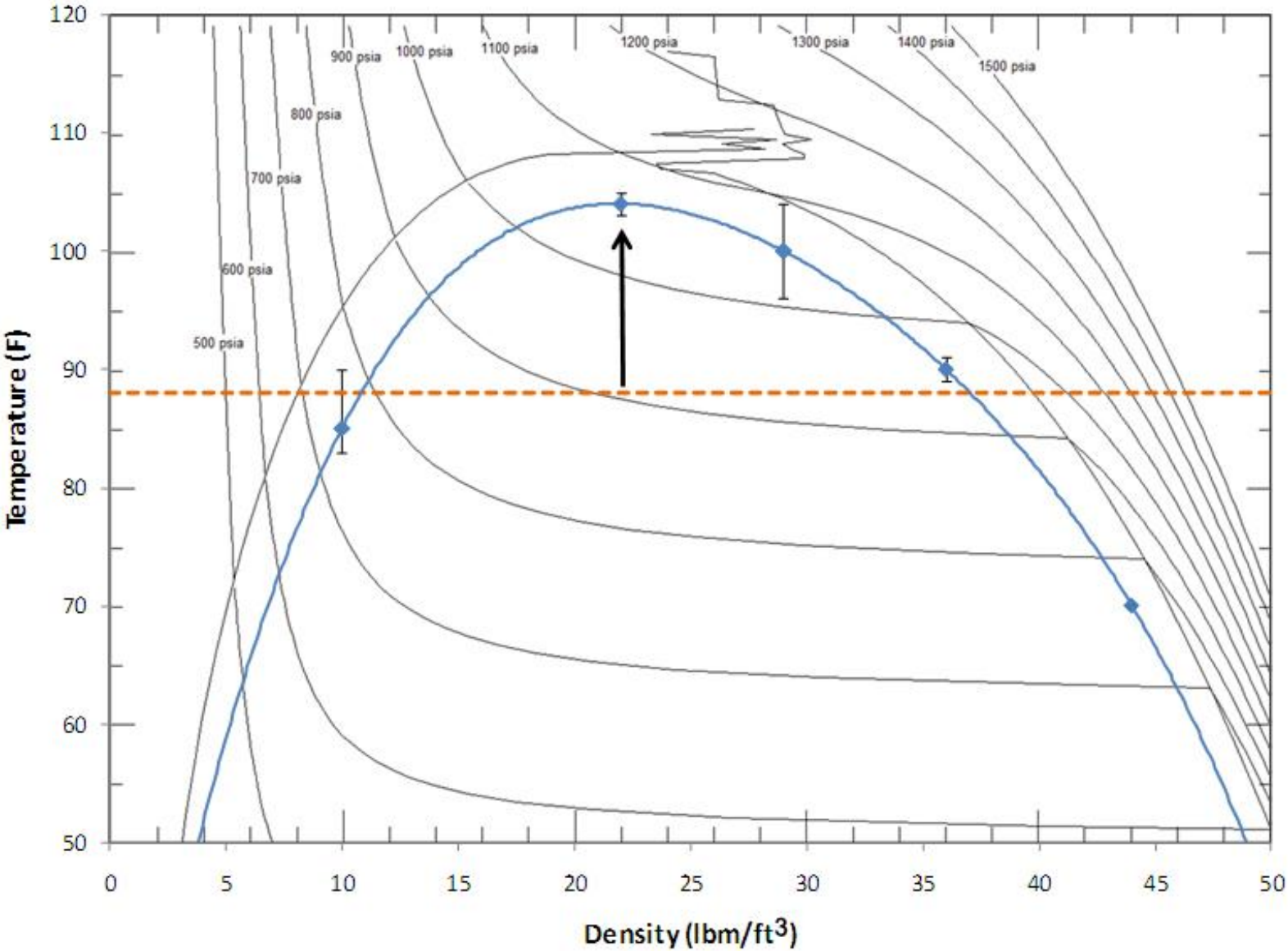

Figure 0-6. Measured and REFPROP predicted saturation curve for schematic of the CO_2/8% butane mixture.

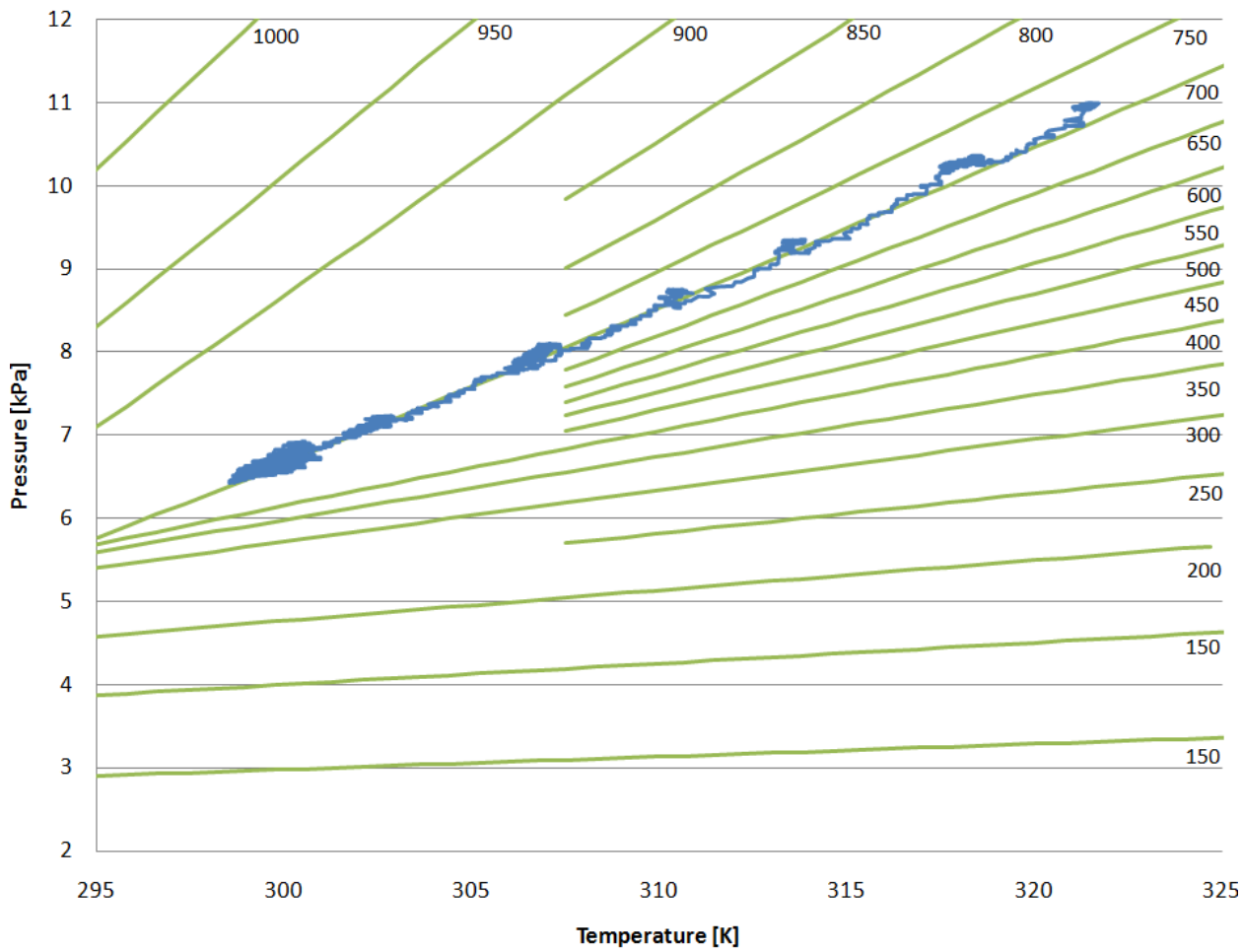

Figure 0-7: The p-T relationship for a 50/50 CO_2/SF_6 mixture at various densities, with experimental data shown at D=700 kg/m^3.

Moreover, during testing, the 50/50 mixture was cooled below even 300 K (80°F) without any observation of mass flow oscillations. Later, literature was found that confirmed that the critical temperature of CO_2/SF_6 mixtures in this ratio drops below that of either pure fluid alone. This is illustrated in Figure 0-8, where the blue and orange curves show NIST models for the CO_2 and SF_6 saturation curves, respectively. Experimental T-ρ data during the cool-down from 320 to 300 K is shown in blue, with cooling past the critical point of CO_2 and no oscillations in mass flow observed (mass flow is not pictured). The black curve shows critical points measured by Diefenbacher [7] at various mixture ratios, and exhibits a downward trend as SF_6 is added to CO_2 in small quantities before finally swinging back up towards higher critical temperatures.

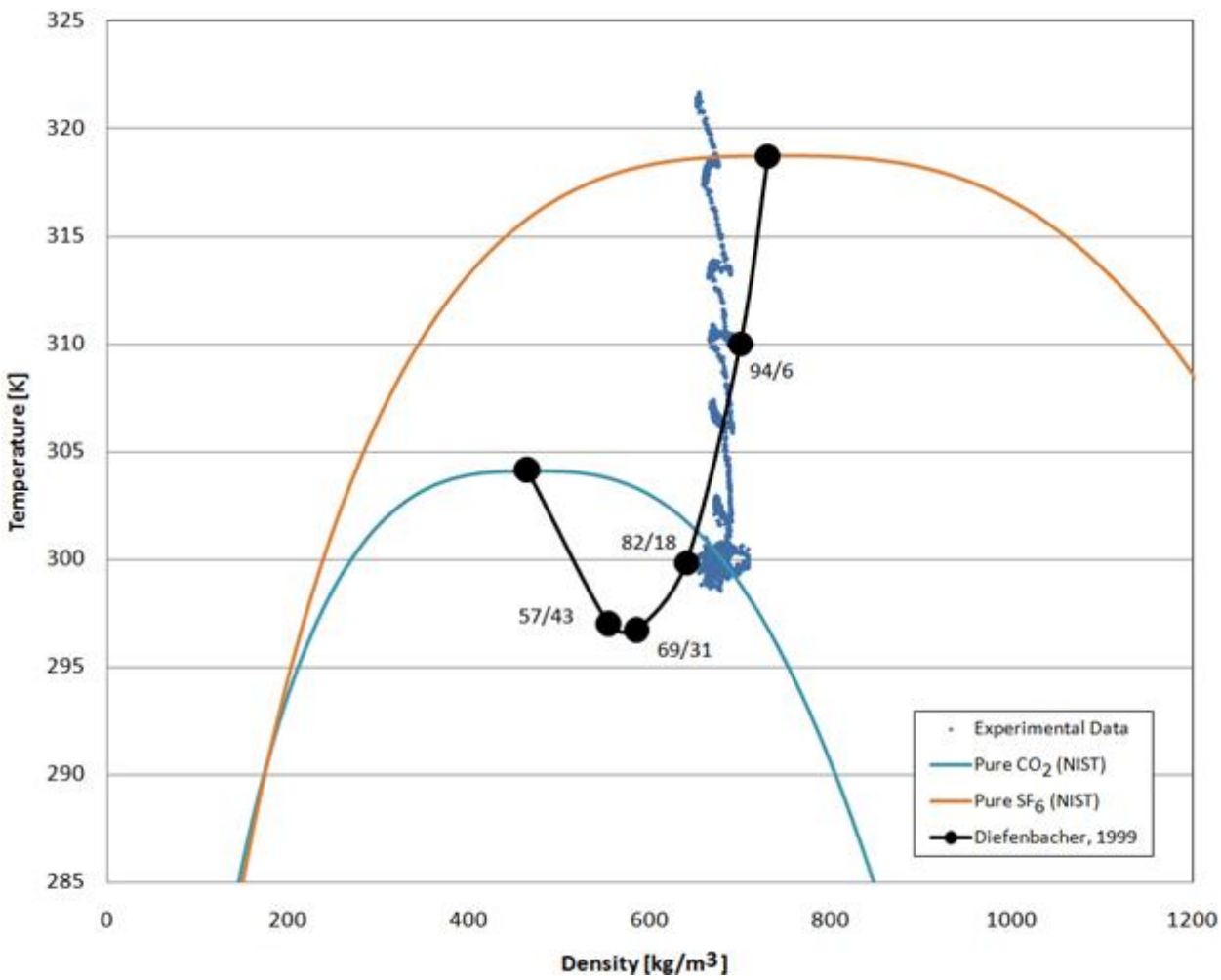

Figure 0-8. A comparison of the T-ρ NIST curves for CO_2 and SF_6, with acquired data.

CO_2/Ne:

As with CO_2/SF_6, REFPROP was fairly accurate in estimating equation of state data for CO_2/Ne but failed to match critical temperature to experimental measurements. Figure 0-9 shows good accuracy in a comparison of experimental pressure versus temperature data for CO_2/4% neon at densities of 20 and 25 lb/ft^3, compared to values from REFPROP, shown as gray solid lines.

As with CO_2/SF_6, NIST has not incorporated a specific model for CO_2/Ne mixtures. Rather, predictions are based on other generalized models [8], and inaccuracies can be expected. Pure neon has a much lower critical temperature than CO_2, at 44K (–380°F); therefore, even a small amount was expected by models to sharply decrease the mixture critical point. In fact, very little change was observed; mass flow oscillations revealed a critical temperature near 303 K (86°F). Data also indicated that the addition of 4% neon noticeably increases the pressure of the critical point from 7.38 MPa (1070 psi) for pure CO_2 to near 9 MPa (1300 psi). These observations were also qualitatively backed up by the findings of a previous experimental study by Lemmon and Jacobsen [9].

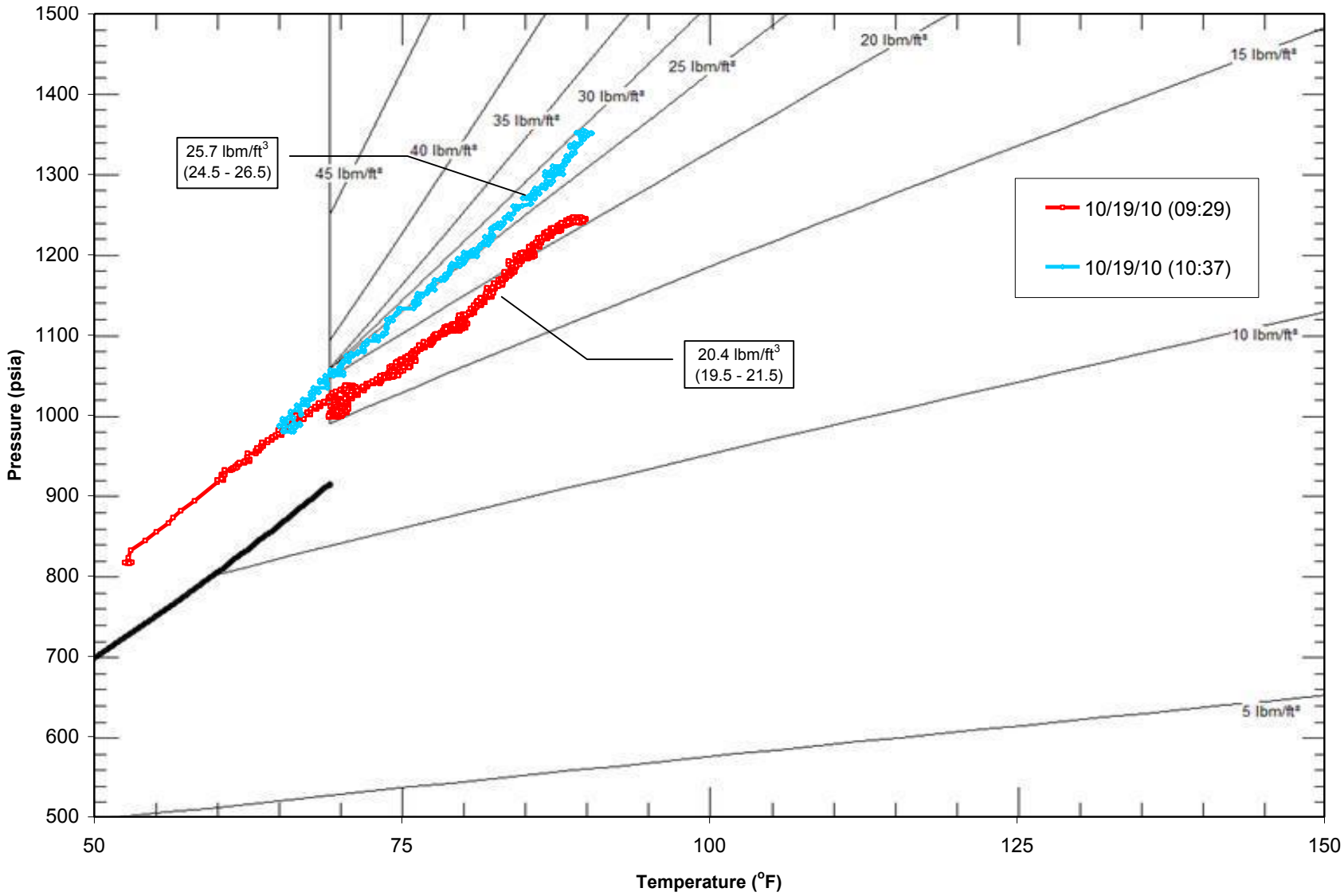

Figure 0-9. Comparison of the p-T data for CO_2/4% Ne at 20 and 25 lb/ft^3 with NIST models.

CONCLUSIONS AND FUTURE WORK

In summary, the research presented in this report used thermodynamic cycle modeling tools to improve the power cycle efficiency of low-temperature geothermal heat sources by using supercritical power cycles. A series of experiments was performed in Sandia's supercritical fluid compression loop that showed that the critical point can be increased or decreased by adding in small quantities of other fluids. The tests first evaluated the compatibility of the new working fluid mixtures with the turbomachinery (screening tests). Several mixtures were tested, including pure CO_2 and then CO_2 with additives of neon, SF_6, and butane.

The improvements in efficiency occur because the supercritical Brayton cycle can be modified to operate well at low temperatures, and because it can take advantage of the nonideal behavior of the supercritical fluid to improve its cycle efficiency. Furthermore, the analysis predicted that certain mixtures using CO_2 and other fluids such as butane or hexane can increase the effective critical point of the fluid, which, in turn, can be used to increase the cycle efficiency at high heat rejection temperatures that will occur when dry cooling is used.

A brief list of the major observations (both measured and modeled) is provided below:

1) An existing cycle analysis code was modified to study a number of low-temperature S-CO_2 power cycles. An optimum cycle that used three stages of reheat and one stage of intercooling in a modified (no high-temperature recuperator) recompression cycle was found to give a cycle efficiency of 18.1% for a turbine inlet temperature of 160ºC and a dry heat rejection temperature of 46.7ºC.
2) In comparison, the same power cycle with pure CO_2 predicted an efficiency of 14.5%. More detailed results show that, at a cooler temperature (305 K), the cycle efficiency can be increased by more than 20%.
3) Screening tests were performed on several mixtures to ensure compatibility with Sandia's supercritical fluid compression loop.
4) The research compressor was operated with three mixtures (Ne, SF_6, and butane mixed with CO_2).
5) The operations measured or estimated the ~~"~~effective" critical point.
6) It was found that SF_6 lowered the critical temperature, and it was confirmed that butane increased the critical temperature.
7) High-speed operations were performed with these mixtures to measure the performance maps for the compressor wheel when operating with the mixtures. These results have not been extensively analyzed. Note that a variety of tools and codes still need to be developed to confirm the applicability and method of ~~"~~translating" the CO_2 maps to maps for other fluids.
8) In all experiment mixtures, tests were performed that demonstrated stable compressor operation in the supercritical region, evidenced by steady, homogenous mass flow and pressure ratio runs at a given compressor speed.
9) Where NIST REFPROP differed from SNL experimental data, this was a result of insufficient data in the existing literature to support accurate mixing parameters.

10) The acquired data is in the process of analysis for the production of nondimensional compressor maps, and for modeling with generalized efficiency/flow coefficient/head coefficient relationships.

Future efforts will focus on developing methods and tools to transform the existing compressor performance maps for CO_2 to the mixtures. For all mixtures, the map data was measured at a variety of shaft speeds but the data has not yet been analyzed. Other modeling efforts will focus on modifying some existing gas-foil thrust bearing modeling tools developed at Sandia to examine the behavior of gas foil bearings using different supercritical fluids. Other future experiments need to be performed with methane and with hexane. Sandia already has the experimental safety approval in place to perform the methane gas mixtures. These tests are particularly important because they offer the ability to improve the power cycle efficiency in colder climates or during winter because methane is predicted to lower the effective critical temperature. The ultimate goal will be to operate Sandia's Brayton cycle at conditions that represent geothermal conditions. Doing this will require some modifications to the turbomachinery so that the turbine and compressor wheels can be designed for the appropriate operating conditions.

REFERENCES

1. L. Qualls et al., *Supercritical Power Conversion Fluid Options for Geothermal Power,* ORNL/SCF/2010-01. Oak Ridge National Laboratory, Oak Ridge, TN, 2010.

2. E. W. Lemmon, M. L. Huber, and M. O. McLinden, NIST Standard Reference Database 23: Reference Fluid Thermodynamic and Transport Properties-REFPROP, Version 9.0. National Institute of Standards and Technology, Standard Reference Database Program, Gaithersburg, MD, 2010.

3. L. Qualls, et al., *Supercritical Power Conversion Fluid Options for Geothermal Power,* ORNL/SCF/2010-01. Oak Ridge National Laboratory, Oak Ridge, TN, 2010.

4. S. Wright, *Optimum Power Cycle Efficiency using 'Tunable' Supercritical Gas Mixtures for Supercritical Brayton Cycles,* Technical Advance #SD11594. Sandia National Laboratories, Albuquerque, NM, 2010.

5. S. Wright and P. Pickard, Supercritical CO_2 Test Loop Operation and First Test Results, in *Proceedings of the International Congress on Advances in Nuclear Power Plants,* Tokyo, Japan, May 10–14, 2009.

6. O. Kunz, R. Klimeck, W. Wagner, and M. Jaeschke, *The GERG-2004 Wide-Range Equation of State for Natural Gases and Other Mixtures,* GERG Technical Monograph 15, Fortschr.-Ber. VDI, VDI-Verlag, Düsseldorf, Germany, 2007.

7. E.W. Lemmon and R.T. Jacobsen, Equations of State for Mixtures of R-32, R-125, R-134a, R-143a, and R-152a, in *J Phys Chem Ref Data,* Vol. 33, No. 2, pp. 593–620, 2004.

8. A. Diefenbacher and M. Turk, Critical (p, ρ, T) Properties of CH_2F_2, $\{xCO_2 + (1-x)SF_6\}$, $\{xSF_6 + (1-x)\ CH_2F_2\}$, and $\{xCH_3 + (1-x)\ CH_2F_2\}$, in *J Chem Thermodyn,* Vol. 31, pp. 905–919, 1999.

9. E. W. Lemmon and R. T. Jacobsen, A Generalized Model for the Thermodynamic Properties of Mixtures, in *Int J Thermophys,* Vol. 20, No. 3, pp. 825–835, 1999.

10. N. V. Kuskova et al., P-ρ-T-c Data for CO_2-Ne Binary Solutions Near the Critical Point of Carbon Dioxide, in *Russ J Phys Chem,* Vol. 57, No. 12, 1983.

Distribution

1	MS0771	Andrew Orrell	6200
1	MS0736	Tito Bonano	6220
1	MS1136	Gary Rochau	6221
1	MS1136	Thomas Conboy	6221
1	MS1136	David Ames	6221
1	MS1136	Tom Lewis	6221
1	MS1136	Steve Wright	6221
1	MS1136	Jim Pasch	6221
1	MS1136	Darryn Fleming	6221
1	MS0899	Technical Library	9536

Sandia National Laboratories